# Seamless Real-Time Precise Point Positioning in Areas without Internet and with Internet

Xiaohan Wang[1], Zhetao Zhang[1,*], Hao Wang[1] and Xinle Pei[1]

[1] School of Earth Sciences and Engineering, Hohai University, Nanjing, 211100, China

**Abstract**

To reduce the cost of real-time high-precision positioning for users, international GNSS service (IGS) and BDS-3 launched the real-time precise point positioning (PPP) service in 2013 and 2020, respectively. IGS provides the services over the internet, while BDS-3 uses the B2b signal from the geostationary earth orbit satellites to offer the service to China and its surrounding areas. IGS state space representation (SSR) and PPP-B2b employ different means of communication and have pros and cons regarding positioning performance and available range. Combining their advantages, this paper proposes a seamless real-time PPP mode to cope with complex communication conditions. Specifically, the mode automatically switches between SSR and B2b messages based on communication availability. When no enhanced message is available, PPP is performed using the broadcast ephemeris (BRDC). First, static positioning experiments are carried out using SSR messages, B2b messages, and BRDC to evaluate their positioning performance. The results indicate that positioning using SSR messages is more accurate and has a shorter convergence time than B2b. Afterward, different communication conditions are simulated, and the performance of the proposed method is verified using a kinematic dataset. Compared to the traditional mode that relies solely on SSR or B2b messages, the seamless PPP mode shows improvements in 3D root mean square error by 20.65% and 10.15%, respectively.

**Keywords**

GNSS, PPP, real-time, communication condition, SSR message, B2b message

## 1. Introduction

As the demand for high-precision positioning grows, positioning technologies based on global navigation satellite systems (GNSS) are becoming more diverse, such as real-time kinematic (RTK) positioning and precise point positioning (PPP) [1]. In recent years, PPP has made significant progress, evolving towards real-time PPP and kinematic PPP applications [2]. To realize real-time PPP, the international GNSS service (IGS) began to provide real-time service (RTS) in 2013, which broadcasts real-time satellite orbit and clock corrections based on state space representation (SSR). At present, some IGS analysis centers provide the products over the internet, such as centre national d'etudes spatiales (CNE), Wuhan university (WHU), etc. Elsobeiey and Al-Harbi described in detail how to use the SSR products [3]. Some scholars compared the performance of SSR products generated by different analysis centers [4, 5, 6]. Li et al. evaluated real-time SSR products, which indicates that the best-quality products are provided by CNE and WHU [6]. Hadas and Bosy analyzed the accuracy of satellite orbit and clock corrections for GPS and GLONASS and proposed a method for predicting corrections [7]. Overall, IGS provides real-time products with orbit accuracy generally better than 5 cm and clock accuracy better than 0.2 ns, which can satisfy most PPP users' positioning needs [4, 5, 6, 7, 8].

The SSR products provided by IGS analysis centers have been thoroughly researched and well applied, but this service is completely dependent on the internet, severely limiting PPP availability. To alleviate this situation, BDS-3, QZSS, and Galileo have launched satellite-based real-time PPP services [9]. In 2020, BDS-3 started to broadcast satellite correction information in and around

Proceedings of the Work-in-Progress Papers at the 14th International Conference on Indoor Positioning and Indoor Navigation (IPIN-WiP 2024), October 14 - 17, 2024, Hong kong, China

* Corresponding author.

xiaohan_wang@hhu.edu.cn (X. Wang); ztzhang@hhu.edu.cn (Z. Zhang); wang_hao@hhu.edu.cn (H. Wang); xinlepei@hhu.edu.cn (X. Pei)

0000-0002-0565-2038 (Z. Zhang)

China through the B2b signal of the geostationary earth orbit (GEO) satellites [10]. In recent years, evaluating the accuracy of B2b products and the performance of positioning with the products has become a hot research topic [11, 12]. Studies have shown that the B2b signal provides orbit and clock corrections with accuracy at the decimeter and centimeter levels, respectively [11]. Ouyang et al. explored the characteristics of B2b messages and evaluated the positioning performance [12]. B2b messages can achieve centimeter-level and decimeter-level positioning accuracy in static and kinematic modes, respectively [12, 13]. Moreover, to further enhance the performance of real-time PPP or realize PPP with ambiguity resolution (PPP-AR), some scholars investigated the use of the BDS short-message communication (SMC) service to convey more enhanced information [14, 15].

Despite correction products based on the B2b signal effectively alleviating the constraints imposed by communication conditions on PPP, the RTS provided by IGS analysis centers still offers advantages, such as update interval and product comprehensiveness. SSR corrections are usually broadcasted with a 5-s interval, while orbit corrections in B2b messages are broadcasted with a 48-s interval. [16]. Tao et al. carefully compared the accuracy of the products from the CNE and PPP-B2b, and the results showed that the B2b message is more accurate for BDS-3 satellites, while the SSR message provided by CNE is more accurate for GPS satellites [17]. In addition, the PPP-B2b service currently supports GPS and BDS-3 satellites, while IGS SSR services typically also provide orbit and clock corrections for GLONASS, Galileo, and BDS-2 satellites.

In summary, both B2b and SSR messages offer distinct advantages and limitations. However, there is a paucity of research on their combined use. To maximize their respective benefits, this paper proposes a seamless PPP mode. Firstly, the methods of using SSR and B2b products are derived, and the seamless PPP mode positioning process is described in detail. Subsequently, static positioning experiments analyze the effects of SSR messages, B2b messages, and broadcast ephemeris (BRDC) on the results. Finally, a vehicle dataset is used to validate the performance of the proposed method under challenging communication conditions.

## 2. Satellite-based Correction Models under Different Communication Conditions

### 2.1. Correction Model Based on SSR Messages Transmitted over the Internet

The real-time SSR products are generated by IGS analysis centers and uploaded to the internet. These products consist mainly of parameters for calculating satellite orbit and clock corrections. The satellite orbit corrections are calculated as follows

$$\begin{bmatrix} \delta O_{rs} \\ \delta O_{as} \\ \delta O_{cs} \end{bmatrix}_t = \begin{bmatrix} \delta O_{rs} \\ \delta O_{as} \\ \delta O_{cs} \end{bmatrix}_{t_0} + \begin{bmatrix} \delta \dot{O}_r \\ \delta \dot{O}_a \\ \delta \dot{O}_c \end{bmatrix} (t - t_0) \tag{1}$$

where $\delta O_{rs}$, $\delta O_{as}$, and $\delta O_{cs}$ represent the satellite orbit corrections in the radial, along-track, and cross-track directions, $\delta \dot{O}_r$, $\delta \dot{O}_a$, and $\delta \dot{O}_c$ the rate of change in the three directions, $t$ and $t_0$ the current and reference epochs, respectively. Since the corrections provided by SSR and B2b messages are based on the satellite-fixed coordinate system. To obtain the corrections in the earth center earth fixed (ECEF) coordinate system, the transformation matrix $\boldsymbol{R}$ is computed as follows

$$\boldsymbol{R} = \left[ \frac{\dot{\boldsymbol{r}}}{|\dot{\boldsymbol{r}}|} \times \frac{\boldsymbol{r} \times \dot{\boldsymbol{r}}}{|\boldsymbol{r} \times \dot{\boldsymbol{r}}|} \quad \frac{\dot{\boldsymbol{r}}}{|\dot{\boldsymbol{r}}|} \quad \frac{\boldsymbol{r} \times \dot{\boldsymbol{r}}}{|\boldsymbol{r} \times \dot{\boldsymbol{r}}|} \right] \tag{2}$$

where $\boldsymbol{r}$ and $\dot{\boldsymbol{r}}$ denote the satellite position and velocity vectors calculated using the BRDC. After that, the real-time precise position of the satellite calculated using the orbit corrections can be represented as follows [7]

$$\begin{bmatrix} X_{SSR} \\ Y_{SSR} \\ Z_{SSR} \end{bmatrix}_t = \begin{bmatrix} X_0 \\ Y_0 \\ Z_0 \end{bmatrix}_t - \boldsymbol{R} \begin{bmatrix} \delta O_{rs} \\ \delta O_{as} \\ \delta O_{cs} \end{bmatrix}_t \tag{3}$$

where $X_{SSR}$, $Y_{SSR}$, and $Z_{SSR}$ denote the corrected satellite coordinates, $X_0$, $Y_0$, and $Z_0$ the satellite coordinates calculated from the BRDC. With the above algorithm, the accuracy of the satellite position can be significantly improved by utilizing the orbit corrections in the SSR messages, i.e., $\delta O_{rs}$, $\delta O_{as}$, $\delta O_{cs}$, $\delta \dot{O}_r$, $\delta \dot{O}_a$, and $\delta \dot{O}_c$.

The clock correction parameters in the SSR messages include three fitting coefficients at the reference epoch, i.e., $C_0$, $C_1$, and $C_2$. The satellite clock correction at the current epoch can be calculated as follows

$$dt_{SSR} = dt_{BRDC} + \frac{C_0 + C_1(t - t_0) + C_2(t - t_0)^2}{c} \tag{4}$$

where $dt_{SSR}$ denotes the corrected satellite clock offset, $dt_{BRDC}$ the satellite clock offset calculated from the BRDC, $c$ the speed of light in a vacuum.

## 2.2. Correction Model Based on B2b Messages Transmitted over the Satellite Telegram

Similar to the SSR messages, B2b messages broadcasted by the BDS-3 GEO satellites also provide correction parameters of satellite orbit and clock offset for BDS-3 and GPS. Furthermore, the B2b message aligns with the CNAV1 message of BDS-3 and the LNAV message of GPS through the issue of data (IOD). The satellite position calculated using the BRDC can be corrected as follows [16]

$$\begin{bmatrix} X_{B2b} \\ Y_{B2b} \\ Z_{B2b} \end{bmatrix} = \begin{bmatrix} X_0 \\ Y_0 \\ Z_0 \end{bmatrix} - \boldsymbol{R} \begin{bmatrix} \delta O_{rb} \\ \delta O_{ab} \\ \delta O_{cb} \end{bmatrix} \tag{5}$$

where $X_{B2b}$, $Y_{B2b}$, and $Z_{B2b}$ denote the corrected satellite coordinates by B2b messages; $\delta O_{rb}$, $\delta O_{ab}$, and $\delta O_{cb}$ express the satellite position corrections provided by B2b messages in the radial, along-track, and cross-track directions.

The satellite clock correction parameters provided by B2b messages are $C_{B2b}$. Afterward, the satellite clock offset can be corrected by

$$dt_{B2b} = dt_{BRDC} - \frac{C_{B2b}}{c} \tag{6}$$

where $dt_{B2b}$ denote the corrected satellite clock offset by B2b messages. The algorithm described above enhances the accuracy and convergence time of real-time PPP in and around China by utilizing the orbit and clock corrections provided in the B2b messages, i.e., $\delta O_{rb}$, $\delta O_{ab}$, $\delta O_{cb}$, and $C_{B2b}$.

## 2.3. Correction Model Combining SSR and B2b Messages

In this section, a seamless PPP mode is proposed to enhance real-time PPP positioning performance in challenging communication environments. Based on current communication conditions, this mode integrates SSR and B2b messages for real-time PPP. Figure 1 shows the flowchart of the seamless PPP mode. The steps filled with blue, yellow, and green denote the input, judgment, and, processing respectively. The entire process can be divided into two main parts: determining communication conditions and using enhanced messages, which are inside the red and purple dotted boxes, respectively. The specific steps are as follows.

Upon receiving real-time GNSS data, the satellite positions and clock offsets are calculated through the BRDC. For instance, the ping command and ConnectivityManager can be used on Linux and Android devices respectively to obtain real-time network connection status. If internet connectivity is stable, the latest SSR messages are obtained, and the delay time is usually no more than the update interval, i.e., 5 s. After that, the satellite-end errors are corrected by (1)-(4) at the current epoch. This process is generally used in densely populated areas with well-developed infrastructure, such as cities.

When the device cannot connect to the network or SSR messages are frequently interrupted, satellite telegraph communication serves as an alternative. Here, it refers to various satellite-based communication services, such as PPP-B2b, BDS-3 SMC, Galileo high accuracy service (HAS), etc. Considering the cost and availability of these services, only PPP-B2b is used in this paper. Since PPP-B2b currently provides corrections only for GPS and BDS-3 satellites, if the receiver tracks these satellites, B2b messages are received and decoded, and the correction program is run according to (5) and (6); otherwise, satellite positions and clock offsets calculated from the BRDC are used for positioning. This positioning procedure is usually used in the wild or where communication facilities are inadequate.

In the worst case, SSR and B2b messages are unavailable, PPP can only be performed using the satellite position and clock offset calculated from the BRDC, i.e., $[X_0\ Y_0\ Z_0]^{\mathrm{T}}$ and $dt_{BRDC}$. Under these circumstances, a well-observed environment is required to achieve convergence of the positioning results, and the results will be worse for shaded scenes. This flow is suitable for areas where neither ground communication base stations nor the B2b signal is available. However, other communication services can compensate if possible, such as BDS-3 SMC, HAS, Starlink, etc. As the user moves between these scenarios, every epoch reassesses the communication conditions to execute the optimal processing flow. The SSR messages, B2b messages, and BRDC seamlessly switch in real time and finally get seamless PPP solutions.

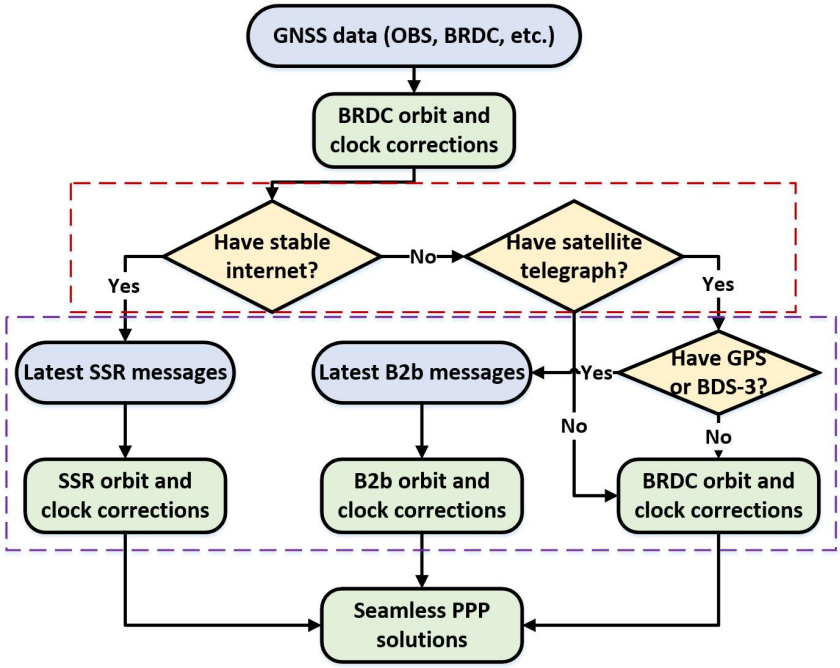


**Figure 1:** Flowchart of the seamless PPP mode.

## 3. Measurement Campaign

Representative static and kinematic experiments were conducted in this study. The GPS and BDS-3 dual-frequency observations (GPS: L1, L2 and BDS-3: B1I, B3I) were collected with a sampling interval of 1 s. For the static experiment, to evaluate the effect of different ephemerides on positioning accuracy and convergence time, a 12-h static dataset on DOY 151, 2023, is used.

For the kinematic experiment, to verify the feasibility of the seamless PPP mode under harsh communication conditions, a 1-s dual-frequency vehicle dataset was collected from P5 manufactured by CHCNAV on DOY 251, 2023. The duration is 5 min and 7 s, and the mean velocity is approximately 27.18 km/h. The kinematic experiment site is located in the urban area of Nanjing, China. As illustrated in Figure 3, the experimental area comprises both open and blocked scenes. The yellow boxes indicate locations where the signal is heavily obstructed and reflected by trees and high-rise buildings.

The kinematic dataset is divided equally into three segments to simulate challenging communication conditions. They can be categorized as both internet and satellite telegraph at 0-102 epochs, only satellite telegraph at 103-204 epochs, and neither internet nor satellite telegraph at 205-306 epochs. Table 1 describes the ephemerides chosen for use by four methods. Method A uses ephemeris without any enhanced products, i.e., BRDC; methods B and C use improved ephemeris by SSR and B2b messages, respectively; and method D seamlessly switches between SSR and B2b messages depending on the communication conditions, i.e., the seamless PPP mode. In addition, BRDC, SSR messages, and B2b messages were saved in advance. In this study, the SSR messages used are generated by the CNE.

**Table 1**
Descriptions of Different Methods Based on the Simulated Communication Conditions

| Method | Ephemeris used at different epochs | | |
|---|---|---|---|
| | 0-102 | 103-204 | 205-306 |
| A | BRDC | | |
| B | SSR | BRDC | |
| C | B2b | | BRDC |
| D | SSR | B2b | BRDC |

## 4. Experimental Tested and Result Analysis

### 4.1. Experiments with Static Datasets

The 12-h high-end receiver dataset was used, collected in a slightly obstructed (southeast) observation circumstance. The number of available satellites with dual frequency observations (GPS: L1, L2 and BDS-3: B1I, B3I) is approximately 15-20, and their geometric dilution precision (GDOP) is stabilized at 1.5 to 2 when the elevation mask is set to 10 degrees.

Figure 2 shows the static PPP positioning errors in east-west (E-W), north-south (N-S), and up-down (U-D) directions using the BRDC, SSR messages, and B2b messages, respectively. It can be seen that the positioning results of the U-D and E-W directions converge slowly, and its positioning error curves fluctuate greatly, especially for the BRDC. It can be clearly seen that the positioning errors and convergence time using SSR and B2b messages are significantly better than those using BRDC. Comparing Figure 2 (b) and (c), it can be noticed that the convergence time using SSR messages is shorter than those using B2b messages. This is mainly due to the higher update frequency of SSR messages transmitted via the internet. The satellite orbit and clock corrections in the SSR messages by CNE are updated with intervals of 5 s. However, in the B2b messages, they are updated with intervals of 48 s and 6 s.

Figure 2 (a) shows that the positioning errors using BRDC have long-term fluctuations at the decimeter level in the U-D direction. Therefore, we defined the convergence criteria of static PPP to be that the positioning errors in the E-W and N-S directions are continuously better than 0.1 m for at least 600 epochs. In order to accurately assess the impact of the three ephemerides on positioning results, Table 2 lists the root mean square error (RMSE) values of all static tests and the horizontal, i.e., E-W and N-S directions, convergence time. It can be seen that the convergence time using BRDC is up to 3.5 h. Compared to the BRDC, the convergence time of the SSR and B2b is shortened by 58.51 and 44.32%, respectively. Moreover, the use of satellite orbit and clock corrections has also greatly improved positioning accuracy. Compared with the BRDC, the 3D RMSE of the SSR and B2b are reduced by 35.78 and 23.48%, respectively.

In short, PPP works best with SSR messages, followed by B2b messages. Furthermore, the SSR messages additionally provide corrections for GLONASS, Galileo, and BDS-2 satellites, thus positioning results based on SSR messages are superior when multi-GNSS observations are used. As a result, when both SSR and B2b messages are available, SSR messages are preferred.

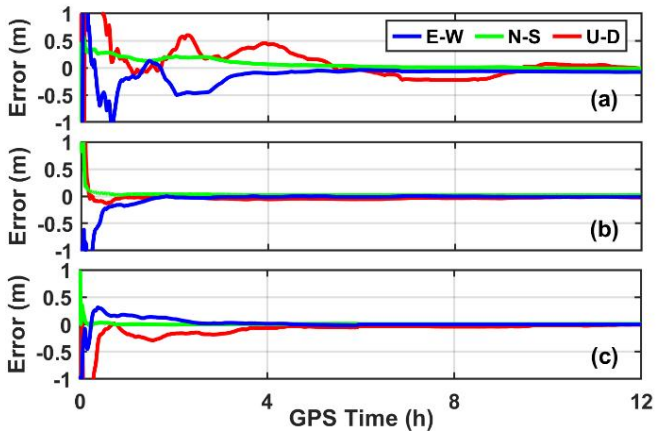


**Figure 2:** Static PPP positioning errors in E (blue), N (green), and U (red) directions by using the BRDC (a), SSR messages (b), and B2b messages (c), respectively.

**Table 2**
Static PPP Positioning Accuracy and Convergence Time Using the Three Ephemeris

| Ephemeris | RMSE (m) | | | 3D (m) | Convergence time (min) |
|---|---|---|---|---|---|
| | E-W | N-S | U-D | | |
| BRDC | 0.361 | 0.117 | 0.498 | 0.626 | 211.083 |
| SSR | 0.115 | 0.028 | 0.384 | 0.402 | 87.583 |
| B2b | 0.193 | 0.090 | 0.428 | 0.479 | 117.533 |

### 4.2. Experiments with Kinematic Datasets

Considering the distribution of ground communication base stations, the communication conditions are related to the user's location, so the seamless PPP mode is mainly applied to kinematic scenarios. In this section, the performance of the seamless PPP mode is carefully analyzed and verified. Based on the four methods listed in Table 1, a seamless PPP experiment with/without the internet is carried out. Figure 3 illustrates the scenario of the experiment site. It can be seen that there are dense buildings and trees around the trajectory, and signals are easily obscured and reflected.

The number of available satellites and the processing of satellite-end errors directly affect the accuracy of PPP. Figure 4 presents the number of satellites corrected using enhanced messages for methods B, C, and D at 0-204 epochs. The receiver is unable to acquire any enhanced messages after 204 epochs, thus the number of satellites corrected by the three methods is 0. Similarly, the internet is unavailable after epoch 102, so the number of satellites corrected by method B is also 0. Statistical analysis of the results in Figure 4 reveals that the mean values of the number of satellites corrected by methods B, C, and D are 5.04, 9.47, and 9.67, respectively. Since SSR messages have better completeness than B2b messages, the seamless PPP mode, i.e., method D, has more satellites with corrected errors than method C.

An analysis combining Figures 3 and 4 finds that the number of available satellites plummets to 5-8 in the two heavily obscured segments, i.e., the area inside the yellow rectangle in Figure 3, which causes a drastic reduction in the accuracy of kinematic PPP. However, the number of corrected satellites remained above 10 most often.

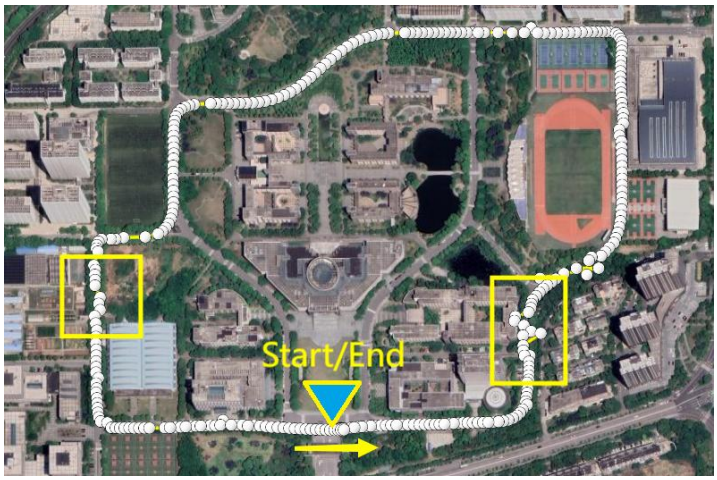


**Figure 3:** Description of kinematic experimental scenarios and trajectory of method A. The yellow boxes denote areas with severe obstruction.

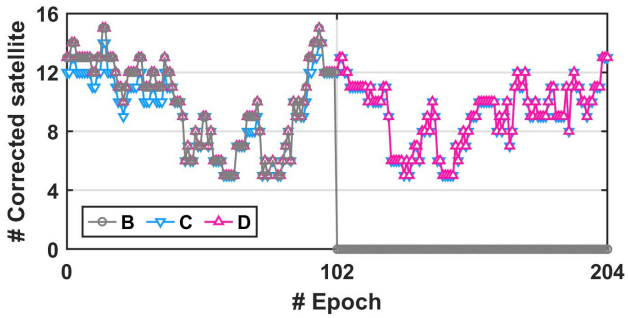


**Figure 4:** Number of corrected satellites for the methods B (grey), C (blue), and D (pink).

To obtain the high-precision reference values, the tight integration of short-baseline RTK and inertial navigation system is applied. The reference station is fixed on the roof of a nearby building with an open sky, and the baseline length is within 1 km throughout the kinematic experiment. To verify the performance of the seamless PPP mode in terms of positioning, Figure 5 (a), (b), (c), and (d) show the positioning results of the methods A, B, C, and D, respectively. The positioning errors in the E-W, N-S, and U-D directions are denoted by blue, green, and red points, respectively. The re-convergences of the positioning results for all four methods can be attributed to complex environments, such as canyon or tree-shaded environments, especially in the U-D direction. A closer look at Figure 5 finds that the positioning results fluctuate dramatically at 55-85 and 222-251 epochs. Combining Figure 5 with Figures 4 and 3 reveals that at these times, the vehicle is heavily shaded, resulting in a reduction in the number of available satellites. Since methods A and B use BRDC for a long time, the results shown in Figure 5 (a) and Figure 5 (b) are less accurate and contain slight bias. Method D fully uses the communication network to obtain the satellite-based corrections, and the horizontal positioning accuracy reaches 1.40 m. According to the communication conditions, methods A, B, C, and D all use BRDC at 204-306 epochs, which caused significant fluctuations in the positioning accuracy in this part.

Table 3 shows the RMSE values of the four methods and the 3D RMSE improvement rates of methods B, C, and D compared to method A. Due to the complexity of the obscuration situations and communication conditions, the positioning accuracy in this experiment is slightly lower than the kinematic PPP in normal scenes. The 3D RMSE values for methods A, B, C, and D are calculated, which are 3.51, 3.06, 2.70, and 2.43 m, respectively. It can be seen that the proposed method D has the most significant 3D RMSE improvement compared to method A, i.e., the BRDC-only method, which is 30.88%. In addition, method D showed an improvement of 20.65 and 10.15% compared to methods B and C with only SSR or B2b messages, respectively. The above results

show that the proposed method D fully utilizes the communication network to improve positioning accuracy under complex communication conditions.

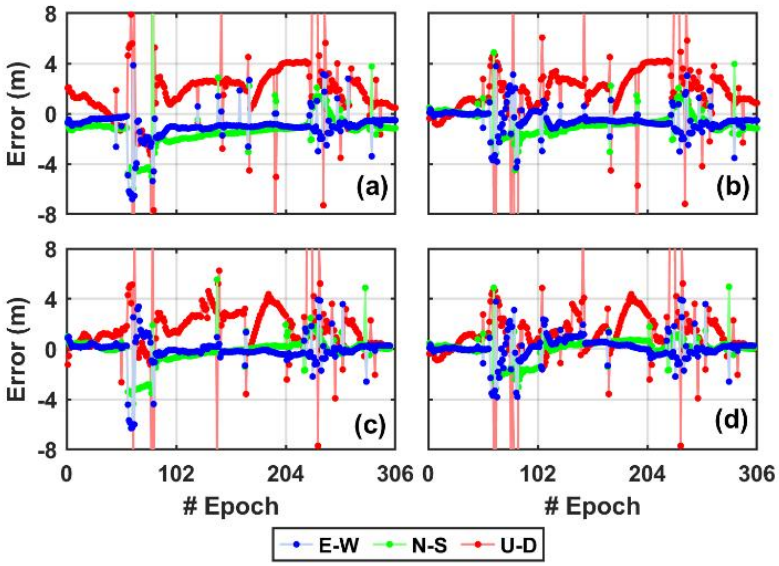


**Figure 5:** Kinematic PPP positioning errors in E (blue), N (green), and U (red) directions by using the methods A (a), B (b), C (c), and D (d), respectively.

**Table 3**
Kinematic PPP Positioning Accuracy and Improvement Rates Using the Four Methods

| Method | RMSE (m) | | | 3D (m) | Improvement rate (%) |
|---|---|---|---|---|---|
| | E-W | N-S | U-D | | |
| A | 1.531 | 1.854 | 2.555 | 3.509 | N/A |
| B | 1.275 | 1.309 | 2.450 | 3.056 | 12.885 |
| C | 1.122 | 1.133 | 2.178 | 2.699 | 23.063 |
| D | 0.978 | 1.010 | 1.976 | 2.425 | 30.878 |

## 5. Conclusion

This paper proposes a seamless PPP mode to alleviate the limitations of communication conditions. Specifically, SSR messages are used in areas covered by the internet; B2b messages are employed when the user moves to an area with poor ground communications; and BRDC is employed for positioning if the communication conditions continue to deteriorate, such as in the wilderness beyond the scope of PPP-B2b service. The static experiments show that positioning accuracy and convergence time are superior when using SSR messages compared to BRDC and B2b messages. Then, the typical kinematic experiments under challenging communication conditions show that compared with the traditional mode using only SSR or B2b messages, the 3D RMSE of the seamless real-time PPP mode is improved by 20.65 and 10.15%, respectively.

In future work, real-time PPP based on the BDS-3 SMC service will be used to improve the BRDC PPP. The PPP-B2b service cannot cover the whole world, so the HAS service will be integrated into the seamless PPP mode.

## Acknowledgments

This study is funded by the National Natural Science Foundation of China (42374014, 42004014), and State Key Laboratory of Geo-Information Engineering and Key Laboratory of Surveying and Mapping Science and Geospatial Information Technology of MNR, CASM (2024-01-07).

## References


[1] J. F. Zumberge, M. B. Heflin, D. C. Jefferson, M. M. Watkins, and F. H. Webb, Precise point positioning for the efficient and robust analysis of GPS data from large networks, J. Geophys. Res 102 (1997) 5005–5017.

[2] X. Zhang, X. Li, and P. Li, Review of GNSS PPP and its application, Acta Geodaetica et Cartographica Sinica 46 (2017) 1399–1407.

[3] M. Elsobeiey and S. Al-Harbi, Performance of real-time precise point positioning using IGS real-time service, GPS Solut 20 (2016) 565–571.

[4] C. Su, B. Shu, and L. Zheng, Quality evaluation and PPP performance analysis of GPS/BDS real-time SSR products, Geomatics and Information Science of Wuhan University (2021) 1-14.

[5] Z. Wang, Z. Li, L. Wang, X. Wang, and H. Yuan, Assessment of multiple GNSS real-time SSR products from different analysis centers, IJGI 7 (2018) 85.

[6] B. Li, H. Ge, Y. Bu, Y. Zheng, and L. Yuan, Comprehensive assessment of real-time precise products from IGS analysis centers, Satell Navig 3 (2022) 12.

[7] T. Hadas and J. Bosy, IGS RTS precise orbits and clocks verification and quality degradation over time, GPS Solut 19 (2015) 93–105.

[8] X. Cao, J. Li, S. Zhang, L. Pan, and K. Kuang, Performance assessment of uncombined precise point positioning using multi-GNSS real-time streams: Computational efficiency and RTS interruption, Advances in Space Research 62 (2018) 3133–3147.

[9] Y. Yang, Y. Mao, and B. Sun, Basic performance and future developments of BeiDou global navigation satellite system, Satell Navig 1 (2020) 1.

[10] R. Hirokawa, I. Fernández-Hernández, and S. Reynolds, PPP/PPP-RTK open formats: Overview, comparison, and proposal for an interoperable message, NAVIGATION 68 (2021) 759–778.

[11] Z. Nie, X. Xu, Z. Wang, and J. Du, Initial assessment of BDS PPP-B2b service: Precision of orbit and clock corrections, and PPP performance, Remote Sensing 13 (2021) 2050.

[12] S. Sun, M. Wang, C. Liu, X. Meng, and R. Ji, Long-term performance analysis of BDS-3 precise point positioning (PPP-B2b) service, GPS Solut 27 (2023) 69.

[13] C. Ouyang, J. Shi, W. Peng, X. Dong, J. Guo, and Y. Yao, Exploring characteristics of BDS-3 PPP-B2b augmentation messages by a three-step analysis procedure, GPS Solut 27 (2023) 119.

[14] Z. Song, J. Chen, Y. Zhang, C. Yu, and J. Ding, Real-time multi-GNSS precise point positioning with ambiguity resolution based on the BDS-3 global short-message communication function, GPS Solut 27 (2023) 136.

[15] K. He, D. Weng, S. Ji, Z. Wang, W. Chen, and Y. Lu, Ocean real-time precise point positioning with the BeiDou short-message service, Remote Sensing 12 (2020) 4167.

[16] R. Lan, C. Yang, Y. Zheng, Q. Xu, J. Lv, and Z. Gao, Evaluation of BDS-3 B1C/B2b single/dual-frequency PPP using PPP-B2b and RTS SSR products in both static and dynamic applications, Remote Sensing 14 (2022) 5835.

[17] J. Tao, J. Liu, Z. Hu, Q. Zhao, G. Chen, and B. Ju, Initial assessment of the BDS-3 PPP-B2b RTS compared with the CNES RTS, GPS Solut 25 (2021) 131.